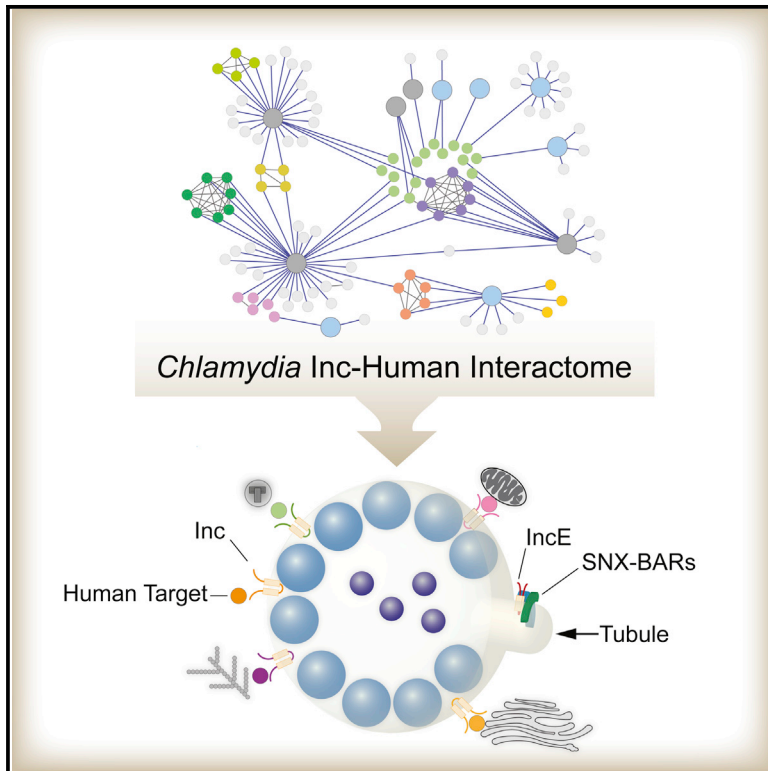


# Cell Host & Microbe

## Global Mapping of the Inc-Human Interactome Reveals that Retromer Restricts *Chlamydia* Infection

### Graphical Abstract



### Authors

Kathleen M. Mirrashidi,  
Cherilyn A. Elwell, Erik Verschueren, ...,  
Raphael Valdivia, Nevan J. Krogan,  
Joanne Engel

### Correspondence

nevan.krogan@ucsf.edu (N.J.K.),  
jengel@medicine.ucsf.edu (J.E.)

### In Brief

*Chlamydia* inclusion membrane proteins are uniquely positioned at the host-pathogen interface, but their host targets are largely unknown. Mirrashidi et al. report a *Chlamydia*-human protein-protein interactome that identifies host proteins and pathways implicated in pathogenesis. They show that *Chlamydia* sequesters retromer components to potentially overcome host mechanisms of pathogen restriction.

### Highlights

- *Chlamydia* inclusion membrane (Inc)-human protein interactions were identified by AP-MS
- Bacterial and viral pathogens share human protein targets
- IncE directly binds the PX domains of retromer components SNX5 and SNX6
- Retromer restricts *Chlamydia* infection and promotes inclusion tubulation



# Global Mapping of the Inc-Human Interactome Reveals that Retromer Restricts *Chlamydia* Infection

Kathleen M. Mirrashidi,<sup>1,9</sup> Cheryl A. Elwell,<sup>1,9</sup> Erik Verschuere,<sup>2,3</sup> Jeffrey R. Johnson,<sup>2,3</sup> Andrew Frando,<sup>1</sup> John Von Dollen,<sup>2,3</sup> Oren Rosenberg,<sup>1</sup> Natali Gulbahce,<sup>2,3</sup> Gwendolyn Jang,<sup>2,3</sup> Tasha Johnson,<sup>2,3</sup> Stefanie Jäger,<sup>2,3</sup> Anusha M. Gopalakrishnan,<sup>4</sup> Jessica Sherry,<sup>1</sup> Joe Dan Dunn,<sup>4</sup> Andrew Olive,<sup>5</sup> Bennett Penn,<sup>1</sup> Michael Shales,<sup>3,6</sup> Jeffery S. Cox,<sup>7</sup> Michael N. Starnbach,<sup>5</sup> Isabelle Derre,<sup>8</sup> Raphael Valdivia,<sup>4</sup> Nevan J. Krogan,<sup>2,3,6,\*</sup> and Joanne Engel<sup>1,7,\*</sup>

<sup>1</sup>Department of Medicine, University of California, San Francisco, San Francisco, CA 94143, USA

<sup>2</sup>QB3, California Institute for Quantitative Biosciences, San Francisco, CA 94148, USA

<sup>3</sup>Department of Cellular and Molecular Pharmacology, University of California, San Francisco, San Francisco, CA 94158, USA

<sup>4</sup>Department of Molecular Genetics and Microbiology, Duke University, Durham, NC 27710, USA

<sup>5</sup>Department of Microbiology, Harvard Medical School, Boston, MA 02115, USA

<sup>6</sup>Gladstone Institutes, San Francisco, CA 94158, USA

<sup>7</sup>Department of Microbiology and Immunology, University of California, San Francisco, San Francisco, CA 94143, USA

<sup>8</sup>Department of Microbial Pathogenesis, Yale School of Medicine, New Haven, CT 06510, USA

<sup>9</sup>Co-first author

\*Correspondence: [nevan.krogan@ucsf.edu](mailto:nevan.krogan@ucsf.edu) (N.J.K.), [jengel@medicine.ucsf.edu](mailto:jengel@medicine.ucsf.edu) (J.E.)

<http://dx.doi.org/10.1016/j.chom.2015.06.004>

## SUMMARY

*Chlamydia trachomatis* is a leading cause of genital and ocular infections for which no vaccine exists. Upon entry into host cells, *C. trachomatis* resides within a membrane-bound compartment—the inclusion—and secretes inclusion membrane proteins (Incs) that are thought to modulate the host-bacterium interface. To expand our understanding of Inc function(s), we subjected putative *C. trachomatis* Incs to affinity purification-mass spectroscopy (AP-MS). We identified Inc-human interactions for 38/58 Incs with enrichment in host processes consistent with *Chlamydia*'s intracellular life cycle. There is significant overlap between Inc targets and viral proteins, suggesting common pathogenic mechanisms among obligate intracellular microbes. IncE binds to sorting nexins (SNXs) 5/6, components of the retromer, which relocalizes SNX5/6 to the inclusion membrane and augments inclusion membrane tubulation. Depletion of retromer components enhances progeny production, revealing that retromer restricts *Chlamydia* infection. This study demonstrates the value of proteomics in unveiling host-pathogen interactions in genetically challenging microbes.

## INTRODUCTION

Intracellular pathogens that replicate within a membrane-bound compartment employ secreted virulence factors to subvert the host and facilitate survival. Decoding these interactions has been especially difficult for genetically challenging organisms, such as *Chlamydiae*. These obligate intracellular pathogens are important causes of human disease for which no effective vac-

cine exists. *C. trachomatis* is the major cause of noncongenital blindness worldwide and a leading cause of sexually transmitted diseases and noncongenital infertility in Western countries (Mandell et al., 2010). *C. pneumoniae* is an important cause of respiratory infections and is linked to a number of chronic diseases (Leonard and Borel, 2014). Although treatable with antibiotics, no drug is cost effective enough for widespread elimination of disease in developing nations.

All *Chlamydiae* share a common intracellular life cycle, alternating between an infectious, spore-like elementary body (EB) and a noninfectious, metabolically active reticulate body (RB) (reviewed in Bastidas et al., 2013). Upon entry into nonphagocytic cells, the EB resides within a membrane-bound compartment—the inclusion—and quickly diverges from the canonical endolysosomal pathway. The EB differentiates into an RB and replication commences. After replicating within the ever-enlarging inclusion over 24–72 hr, the RB redifferentiates to an EB and is then released, ready to infect neighboring cells.

How *Chlamydia* establishes its replicative niche is incompletely understood. *Chlamydia* manipulates the actin cytoskeleton and microtubule-based motors; obtains nutrients; interacts with numerous host cell organelles; and inhibits the innate immune system, autophagy, and programmed cell death (Bastidas et al., 2013). However, the *Chlamydia* factors and host cell proteins that mediate these events are largely unknown.

Despite their small genome size, *Chlamydia* are estimated to encode a disproportionate number of secreted virulence effectors, ~10%–15% of their genome (Betts-Hampikian and Fields, 2010). A large subset of effectors, termed inclusion membrane proteins (Incs), are translocated by the type III secretion system and inserted into the inclusion membrane (Moore and Ouellette, 2014). Their defining feature is the presence of one or more unique bilobed domains, typically composed of two closely spaced transmembrane regions separated by a short loop (Bannantine et al., 2000) (Figure 1A). Once inserted into the inclusion membrane, Incs are predicted to extend their termini into the host cytoplasm (Rockey et al., 2002), ideally positioning them at the host-pathogen interface. Given the only recent and

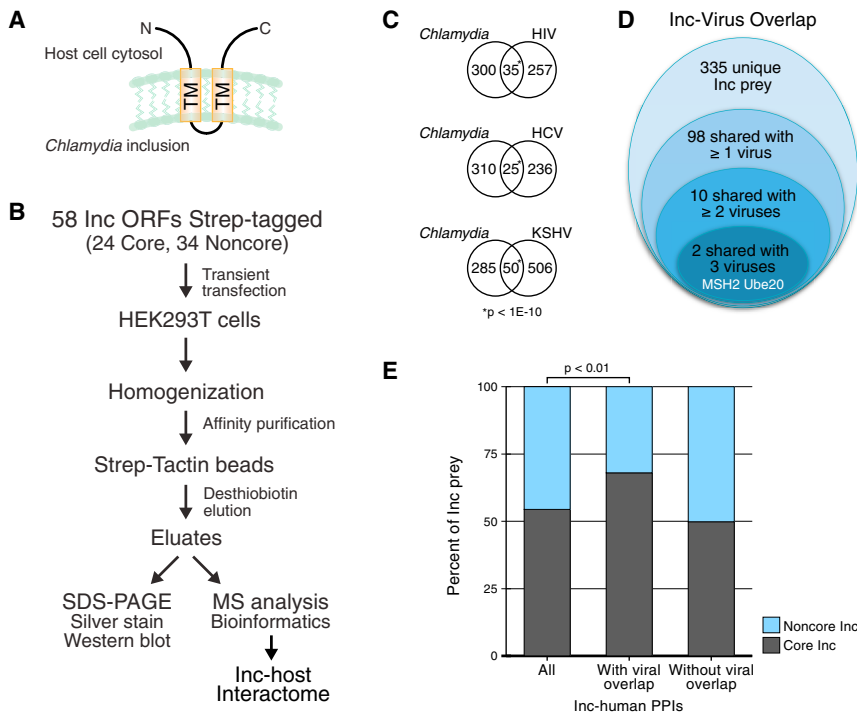


**Figure 1. Constructing the *Chlamydia* Inc-Human Interactome**

(A) Predicted topology of Inc proteins in the *Chlamydia* inclusion membrane.

(B) Workflow summary.

(C) Overlap of *Chlamydia* prey with previously published AP-MS interactomes of HIV (Jäger et al., 2012), HCV (Ramage et al., 2015), and KSHV (Davis et al., 2015). p values were determined by the hypergeometric test.

(D) Number of prey shared between *Chlamydia* Incs and viral interactomes.

(E) Bar graph depicting the percentage of Inc prey. For the prey identified for 38 Inc constructs (“All”), 56% of prey were affinity purified by core Inc, while 44% of prey were affinity purified by noncore Inc. Of the 98 prey shared by *Chlamydia* Inc and one or more virus (“with viral overlap”), there was a statistically significant increase in core Inc that overlap with viral prey (68%) versus noncore Inc (32%). There was no significant change in the percentage of prey bound to core versus noncore Inc for the 237 prey not shared with viruses (“without viral overlap”). p < 0.01 determined by the hypergeometric test. See also Figure S1, Table S1, and Table S3.

limited ability to genetically modify *Chlamydia*, a detailed understanding of the roles of Inc during infection has been challenging. Indeed, only a few host-binding partners of Inc have been identified (Moore and Ouellette, 2014). Furthermore, Inc share little homology to each other or to known proteins, providing limited insight to their functions (Dehoux et al., 2011; Lutter et al., 2012).

We used large-scale AP-MS to comprehensively identify protein-protein interactions (PPIs) between *C. trachomatis* Inc and the host proteome to decode mechanisms by which this pathogen establishes its privileged intracellular niche. Our analysis has uncovered a wealth of previously unidentified *Chlamydia* Inc-host interactions. We analyzed in detail the interaction between IncE, an early expressed Inc of unknown function, and the SNX-BAR proteins, a subset of retromer components. We found that IncE directly binds the PX domains of SNX5/6, that IncE is sufficient to disrupt retromer trafficking, and that retromer restricts *C. trachomatis* infection. Our study underscores the power of using comprehensive proteomics to study host-pathogen interactions, particularly for genetically challenging organisms such as *Chlamydia*.

## RESULTS

### AP-MS Identifies High-Confidence Inc-Human PPIs

We cloned nearly all (58) of the 62 predicted *C. trachomatis* Inc (Dehoux et al., 2011; Lutter et al., 2012) from two *C. trachomatis* ofeomes (Roan and Stambach, 2006; Sisko et al., 2006), including the full-length proteins and/or the predicted cytoplasmic domains. Twenty-four of these Inc are evolutionarily conserved among five or more *Chlamydia* species (“core” Inc) (Dehoux et al., 2011; Griffiths et al., 2006; Lutter et al., 2012). A total of 78 Inc constructs were fused to Strep tags, tran-

siently expressed in HEK293T cells, and affinity purified (AP) over Strep-Tactin beads. Entire eluates were subjected to MS (Figure 1B). All APs were performed in at least triplicate and confirmed by immunoblotting with an anti-Strep antibody and silver staining (data not shown). From over 250 AP-MS runs, we identified 30,924 PPIs (see Table S1 available online), representing 2,982 unique human proteins.

A set of high-confidence PPIs was established by analyzing the complete data set using two algorithms: MiST (Jäger et al., 2012) and CompPASS (Sowa et al., 2009) (Table S1). Using stringent criteria (MiST score  $\geq 0.7$  or the top 1% of CompPASS scores), we identified 354 high-confidence Inc-human PPIs, representing 335 unique host binding partners for 38/58 Inc (Table S1; Figure S1). Importantly, IncD and CT228 coeluted their known human targets, CERT (Derré et al., 2011) and MYPT1 (Lutter et al., 2013), respectively, as the highest-confidence PPI (Table S1). These findings establish the validity of our scoring system and demonstrate that our pipeline correctly identifies biologically confirmed PPIs for transmembrane proteins such as the Inc.

### Constructing a Comprehensive Inc-Human PPI Network

We assembled an Inc-human PPI network using two databases of known human-human protein interactions (CORUM [Ruepp et al., 2010] and STRING [Franceschini et al., 2013]) to identify multiprotein complexes and potential connections between Inc (Figure 2). Within this subset, we found individual Inc that associate with several members of multiprotein complexes, including retromer, COP9 signalosome, condensin II, GINS, and dynactin. We also observed numerous examples of two or more individual Inc that interact with the same host complex. For example, five Inc (CT005, CT556, CT195, CT058, and CT819) interacted with members of the TIM-TOM complex,

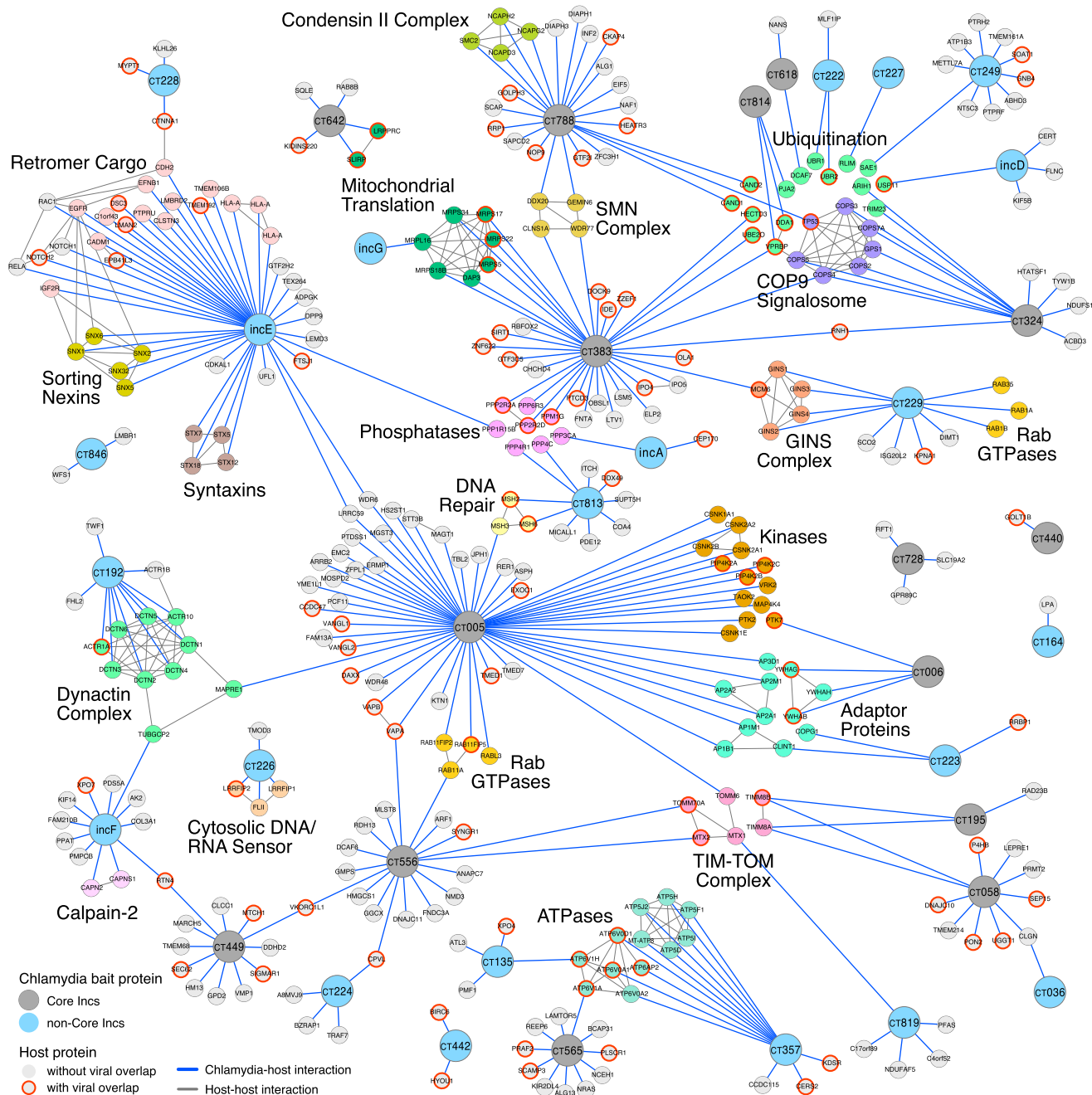


**Figure 2. Network Representation of the Inc-Human Interactome**

The high-confidence Inc-host network contains 38 Inc proteins (core Inc proteins, dark gray; non-core Inc proteins, light blue), and 335 unique human prey (light gray). Inc-human interactions (blue lines) were identified by AP-MS. Interactions between human proteins (dark gray lines) were curated from CORUM and STRING databases. Inc-human prey in common with HIV, KSHV, or HCV prey (Davis et al., 2015; Jäger et al., 2012; Ramage et al., 2015) are outlined in red. A subset of identified host complexes or proteins with similar functions are labeled. See also Table S2.

host machinery responsible for mitochondrial protein import (Bauer et al., 2000). Three Inc proteins (CT135, CT565, and CT357) each bind to different subunits of vacuolar ATPases, multiprotein enzymes that control acidification of intracellular organelles (Marshansky and Futai, 2008). We also identified several Inc proteins that target proteins involved in ubiquitination, consistent with a

recent report that *C. trachomatis* remodels the host proteome (Olive et al., 2014). Finally, we found a subset of host proteins (RTN4, VKORC1L1, CPVL, LRRC59, WDR6, VPRBP, and RNH1) that were each targeted by two individual Inc proteins, suggesting that modulating these targets may be critical for *Chlamydia*'s intracellular survival.

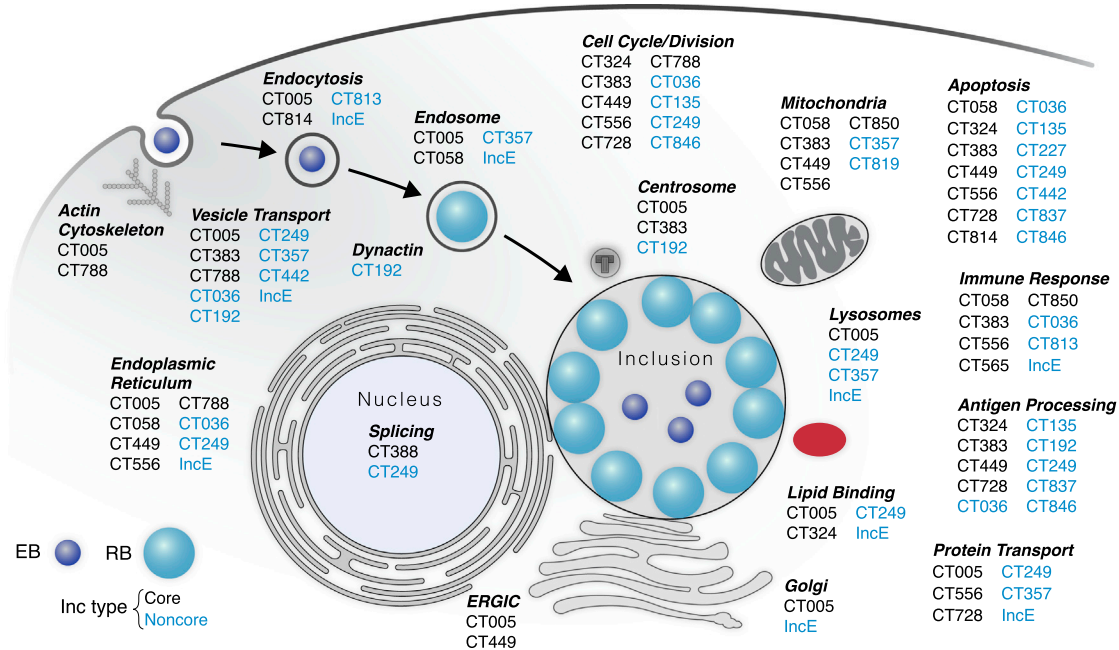


**Figure 3. Predicted Functions for Specific IncRNAs**

Schematic diagram of the *Chlamydia* developmental cycle, indicating predicted functions of putative IncRNAs derived from GO, KEGG, and PFAM enrichment terms from the entire PPI data set (see Table S2). Core IncRNAs, black; Noncore IncRNAs, blue. Note that some predicted IncRNAs have not been observed on the inclusion membrane at 24 hpi (Li et al., 2008, Dehoux et al., 2011). See also Table S1 and Figures S2 and S3.

### The Inc-Human Interactome Predicts Inc Functions during *Chlamydia* Development

Analysis of the entire data set with gene ontology (GO) and protein database (KEGG and PFAM) terms revealed that Inc-host protein interactions were enriched for many compartments and pathways consistent with *Chlamydia*'s intracellular life cycle (Figures 3, S2, and S3; Table S2). For example, we found increased representation for host proteins that localize to the ER, Golgi, mitochondria, endosomes, lysosomes, and actin cytoskeleton, all of which associate with the *C. trachomatis* inclusion (Bastidas et al., 2013). We also identified host targets enriched for biological processes and molecular functions known to be modulated during infection, such as endocytosis, ubiquitination, apoptosis, cell cycle/division, and DNA damage/repair (Bastidas et al., 2013).

Our analysis uncovered cellular processes that may be modulated by *Chlamydia*, such as chromosome condensation (Condensin II complex), splicing (SMN complex), retromer trafficking (SNXs), and the cytosolic surveillance response (DNA/RNA sensors) (Figures 2, S2, and S3; Table S2). Our PPI data set allows us to now link specific IncRNAs to host cell processes important for infection (Figure 3).

### Chlamydial and Viral Effectors Share Host Protein Targets

To determine whether diverse intracellular pathogens target host proteins in common with each other, we compared our Inc-human interactome to three recently assembled virus-human interactomes: HIV (Jäger et al., 2012), KSHV (Davis et al., 2015), and HCV (Ramage et al., 2015). These viral interactomes were derived using the same pipeline that we employed, providing

an opportunity for cross-pathogen analyses. We found a significant overlap in high-confidence prey between *Chlamydia* and each of the three viruses (Figure 1C; Table S3). We identified 98 high-confidence *C. trachomatis* prey shared with one or more viruses, 10 shared with 2 or more viruses, and 2 shared with all 3 viruses (Figure 1D). Host complexes or pathways targeted by *Chlamydia* and one or more viruses included lysosomal ATPases, DNA repair, the TIM-TOM complex, the dynactin complex, the ubiquitin machinery, and Golgi trafficking (Figure 2). Strikingly, we found core IncRNAs were more likely to overlap with viral targets compared to non-core IncRNAs ( $p < 0.001$ ; Figure 1E; Table S3).

### IncE Interacts with Retromer-Associated Sorting Nexins

Our interactome revealed that IncE was enriched for retromer-associated proteins, including SNX1, SNX2, SNX5, and SNX6 (SNX1/2/5/6) (Figures S2 and 2; Table S2). IncE, located in an operon together with IncD, IncF, and IncG, is expressed within the first 2 hr of *C. trachomatis* infection (Scidmore-Carlson et al., 1999), but its function(s) and host binding partners were unknown. The retromer complex is composed of the vacuolar protein sorting (VPS) trimer and a heterodimer of SNX-BAR proteins, SNX1/2-SNX5/6 (Cullen and Carlton, 2012; Teasdale and Collins, 2012). SNX-BAR proteins are comprised of a phosphoinositide-binding Phox homology (PX) domain, which functions in endosomal membrane trafficking, membrane remodeling, and organelle motility (Cullen and Korswagen, 2012; Seaman, 2012), and a Bin-amphiphysin-Rvs (BAR) domain, which both senses and induces membrane curvature (Teasdale and Collins, 2012). By inducing tubulation and then recruiting additional factors that lead to scission and

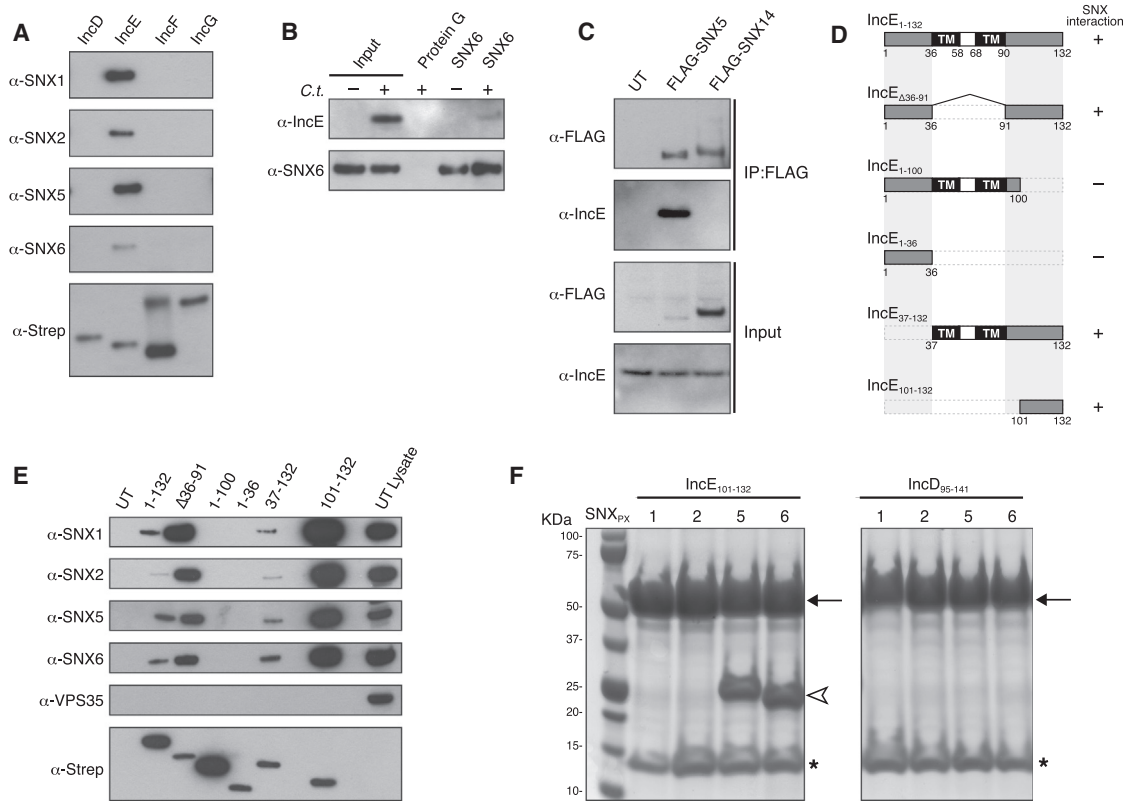


**Figure 4. IncE Interacts with Retromer SNX-BARs In Vivo and In Vitro**

(A) Affinity purifications of HEK293T cells transiently expressing Strep-tagged IncE and immunoblotted with the indicated antibodies.

(B and C) IncE interacts with endogenous SNX6 (B) and transiently expressed SNX5-FLAG (C) in vivo. Immunoblot analysis of immunoprecipitations with anti-SNX6, anti-FLAG, or anti-goat IgG in HeLa cells uninfected (–) or infected (+) with *C. trachomatis* (C.t.) for 24 hr. Input represents 1% of lysates used for immunoprecipitation. Immunoblots are representative of  $\geq 3$  independent experiments. Untransfected, UT.

(D) Schematic of IncE deletion constructs. The predicted transmembrane (TM) domains are shaded in black; the predicted N- and C-terminal cytosolic domains are shaded in gray. The numbers refer to amino acids. Constructs that coaffinity purify with SNX-BARs are indicated.

(E) Affinity purifications of Strep-tagged IncE deletion constructs transiently expressed in HEK293T cells.

(F) IncE<sub>101–132</sub> binds the PX domains of SNX5 and SNX6 in vitro. Purified 6xHis-MBP-IncE-Strep protein was immobilized to Strep-Tactin beads and incubated with the indicated purified 8xHis-SNX<sub>PX</sub>, subjected to SDS-PAGE, and visualized by Coomassie blue stain. Arrow, IncE or IncD. Arrowhead, SNX<sub>PX</sub>. Asterisk, Strep-Tactin. Molecular weight markers are indicated. See also Figure S4.

formation of vesicles, the retromer SNX-BARS facilitate sorting of protein receptors between endosomes and the *trans*-Golgi network (Cullen and Carlton, 2012; Seaman, 2012). All four retromer SNX-BARs (SNX1/2/5/6) were identified as very-high-confidence targets of IncE (MiST > 0.96; top 0.002% of CompPASS) (Table S1).

We confirmed that IncE interacts specifically with retromer SNX-BARs in vivo. Endogenous retromer SNX-BARs coaffinity purified with transiently expressed IncE, but not IncD, IncF, or IncG (Figures 4A and S4A). In *C. trachomatis*-infected cells, IncE coimmunoprecipitated with endogenous SNX6 (Figure 4B) or with transfected FLAG-SNX5, but not transfected FLAG-SNX14 (Figure 4C), revealing that IncE specifically binds SNX5/6 in vivo.

We tested informative deletion mutants of IncE-Strep (Figure 4D) by transient expression in HEK293T cells and found that only mutants containing the IncE C-terminal cytoplasmic domain (IncE<sub>101–132</sub>) coaffinity purified with retromer SNX-BARs (Figures 4E and S4B). AP-MS of IncE<sub>101–132</sub> also identi-

fied retromer SNX-BARs as the highest confidence PPIs (Table S1). Finally, IncE<sub>101–132</sub>-EGFP colocalized with endogenous SNX1, SNX2, SNX6, and transiently expressed FLAG-SNX5 in endosomes, as visualized by confocal microscopy (Figure S4C). Together, these results show that IncE<sub>101–132</sub> is both necessary and sufficient to interact specifically with retromer SNX-BARs.

#### IncE<sub>101–132</sub> Binds Directly to the PX Domains of SNX5 and SNX6

To determine whether IncE<sub>101–132</sub> binds directly to one or more retromer SNX-BARs, we performed in vitro pull-downs with 6xHis-MBP-IncE-Strep and 8xHis- or 6xHis-MBP-SNXs individually purified from *E. coli*. IncE<sub>101–132</sub> directly bound to the PX domains of SNX5 and SNX6, but failed to bind the corresponding PX domains of SNX1 or SNX2. The C-terminal cytoplasmic domain of IncD, IncD<sub>95–141</sub>, did not bind the PX domains of retromer SNX-BARs (Figure 4F). Neither IncE<sub>101–132</sub> nor IncD<sub>95–141</sub> bound the BAR domains of retromer SNX-BARs in vitro

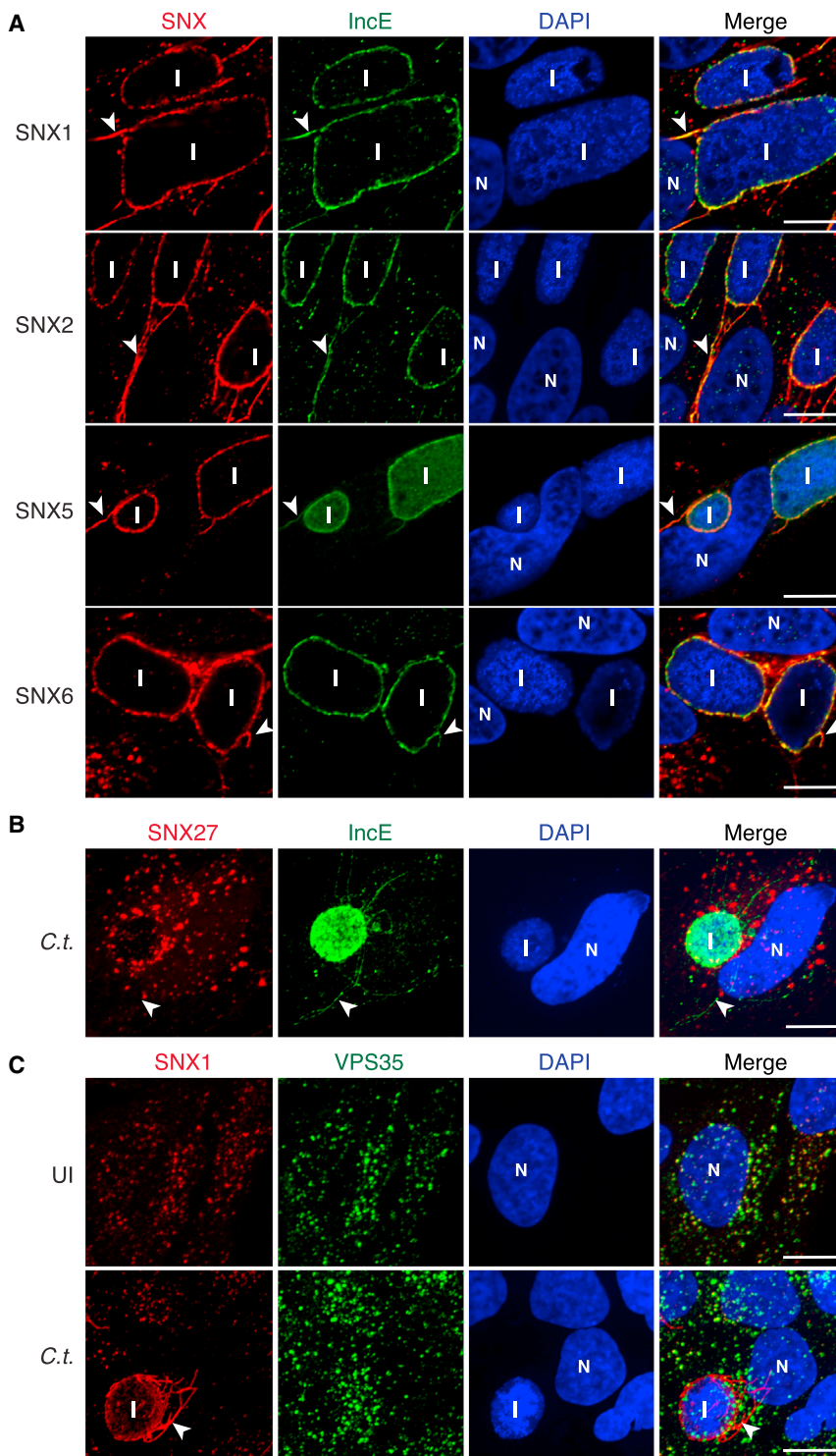


### Figure 5. IncE Colocalizes with Retromer SNX-BARs on the Inclusion

(A–C) HeLa cells were infected with *C. trachomatis* (*C.t.*) for 24 hr and analyzed by confocal microscopy for the localization of (A) endogenous SNX1/2/6 or transfected SNX5-FLAG and IncE, (B) SNX27-EGFP (pseudocolored red) and IncE, or (C) endogenous SNX1 and VPS35. Panels are (A) single z slices or (B and C) maximum intensity projections of 0.3  $\mu\text{m}$  z slices. I, inclusion. N, nucleus. UI, uninfected. Arrowheads point to tubules. Scale bar, 10  $\mu\text{m}$ . See also Figure S5.

suggesting that this secondary structure may play a role in the direct binding of IncE to SNX5/6.

### Retromer SNX-BARs Colocalize with IncE on the Inclusion Membrane

Retromer SNX-BARs primarily colocalize with PtdIns(3)-rich endosomal membranes (Cullen and Carlton, 2012; Seaman, 2012). Confocal microscopy of *C. trachomatis*-infected cells stained with antibodies to SNXs and to IncE revealed that at 6 and 24 hr postinfection (hpi), endogenous SNX1, SNX2, SNX6, and transfected FLAG-SNX5 colocalized with IncE on the inclusion membrane (Figures 5A, S5B, and S5C; data not shown). We also observed IncE on tubules emanating from inclusions that were positive for SNX1, SNX2, FLAG-SNX5, SNX6, and IncA (Figures 5A and S5A–S5C). In contrast, SNX27, a retromer-associated SNX involved in endosome-to-plasma membrane cargo recycling (Lauffer et al., 2010), was not recruited to the inclusion, but instead remained localized in punctate structures (Figures 5B). Thus, *Chlamydia* inclusions and tubules specifically associate with retromer SNX-BARs.

Retromer functions in trafficking cargo-containing vesicles along microtubules to the *trans*-Golgi through the interaction of SNX6 with dynactin subunit 1 (Hong et al., 2009). To determine whether *Chlamydia* inclusion tubulation requires microtubule polymerization, infected cells were exposed to nocodazole, and tubules were examined by confocal microscopy. Microtubules were required for

(Figure S4D). Thus, IncE<sub>101–132</sub> is sufficient to bind SNX5/6 PX domains in the absence of other human proteins. PSIPRED protein sequence analysis revealed that IncE<sub>101–132</sub> contains a putative  $\beta$ -hairpin structure (Figure S4E). In vitro pull-downs of IncE<sub>101–132</sub> truncations (Figure S4E) demonstrated that the  $\beta$ -hairpin region was required for SNX5 binding (Figure S4F),

the formation of SNX and IncE-positive tubules at 6 hpi (Figure S5B) and 24 hpi (Figure S5C). However, microtubule polymerization was not required for SNX recruitment to inclusions (Figures S5B and S5C), consistent with our results demonstrating that IncE directly binds to and likely recruits SNX5/6 to the inclusion.

### Chlamydia Inclusions Do Not Stably Associate with the VPS Subcomplex

In addition to SNX heterodimers, retromer also contains the tripartite cargo recruitment complex composed of VPS26A, VPS29, and VPS35 (Seaman, 2012). While retromer SNX-BARs co-affinity purified with IncE, the VPS subunits and other retromer-associated SNXs were notably absent (Table S1; Figure 4E). Confocal microscopy of *C. trachomatis*-infected cells demonstrated that, in contrast to the robust recruitment of SNX-BARs to the inclusion membrane, VPS35 (Figure 5C) and GFP-VPS29 (data not shown) remained in punctate structures. *Chlamydia* infection significantly diminished SNX1 localization to VPS35-positive compartments (Figure S5D,  $p < 0.0001$ ), while total protein levels were unchanged (Figure S5E), suggesting that *Chlamydia* relocalizes SNX-BARs from endosomes to the inclusion membrane.

SNX1 is recruited to early *Salmonella*-containing vacuoles (SCVs) (Bujny et al., 2008), so we assessed whether other retromer components are recruited to SCVs. We confirmed SNX1 recruitment (Figure S5F) and also found that SNX2 and VPS35 clearly decorated SCVs and associated tubules (Figures S5G and S5H). Thus, in contrast to endosomal membrane tubules or SCVs, *Chlamydia* inclusions and tubules do not maintain a stable association with the VPS complex.

### IncE Is Sufficient to Recruit Retromer SNX-BARs and Induce Inclusion Tubulation

BAR domain-containing proteins form a helical coat, which impose membrane curvature and remodel membranes into tubular profiles (Frost et al., 2008). Based on our observation that retromer SNX-BARs colocalized with IncE on *Chlamydia* inclusion membrane tubules, we predicted that overexpression of IncE would be sufficient to enhance inclusion tubulation. Therefore, we transformed *C. trachomatis* serovar L2, a strain with lower baseline levels of tubulation compared to serovar D, with plasmids engineered to express C-terminally FLAG-tagged IncE (pTet-IncE-FLAG) or IncG (pTet-IncG-FLAG) under a tetracycline (Tc)-inducible promoter. As expected, upon induction with Tc, IncE-FLAG and IncG-FLAG were readily detected on the inclusion membrane and tubules (Figure 6A). Importantly, induction of IncE-FLAG was sufficient to enhance recruitment of SNX6 to the inclusion (Figures 6B and 6C) and to enhance formation of IncA-positive (Figure S6A) and SNX6-positive (Figure 6C) tubules compared to IncG-FLAG or uninduced controls. We also observed increased SNX6 recruitment and SNX6-positive tubules in *C. trachomatis* transformed with a vector expressing untagged IncE (pIncE) under control of its native promoter compared to *C. trachomatis* transformed with empty vector (Figures 6D and 6E). IncE expression in *C. trachomatis*-transformed strains was verified by immunoblot analysis (Figures S6B and S6C). We conclude that IncE expression is sufficient to enhance SNX6 inclusion recruitment and inclusion tubulation.

We used siRNA depletion to determine if retromer function is required for inclusion tubulation. Due to functional redundancy of retromer SNX-BARs (Seaman, 2012), we simultaneously depleted cells of SNX1 and SNX2, SNX5, and SNX6; all four SNXs; or VPS35 (Figure S6D). Depletion of any retromer component decreased both the length and number of inclusion tubules

(Figures 6F and S6E), consistent with our model that recruitment of SNX-BARs enhances inclusion tubulation.

### IncE Disrupts Retromer-Dependent Trafficking of the Cation-Independent Mannose-6-Phosphate Receptor

Since IncE bound SNX5/6 in vitro (Figure 4F), and *C. trachomatis* infection caused relocalization of SNX5/6 from endosomes to the inclusion membrane (Figures 5A), we tested whether IncE could interfere with retromer-dependent trafficking. For these experiments, we transfected cells with IncE<sub>101–132</sub>-EGFP, or, as a control, IncD<sub>95–141</sub>-EGFP, and analyzed localization of the retromer trafficked cation-independent mannose-6-phosphate receptor (CI-MPR), a well-established assay for retromer function (Arighi et al., 2004; Wassmer et al., 2007). Compared to untransfected cells or transfection with IncD<sub>95–141</sub>, transfection with IncE<sub>101–132</sub>-EGFP changed the distribution of CI-MPR from juxtannuclear TGN46-positive compartments to a more disperse collection of large vesicles (Figure 7A). Concomitantly, there was decreased colocalization between CI-MPR and TGN46 (Figure 7B). Instead, CI-MPR largely overlapped with VPS35 and IncE<sub>101–132</sub>-EGFP (Figure 7C), indicating that IncE<sub>101–132</sub>-EGFP expression is sufficient to maintain CI-MPR in retromer-containing compartments, thereby disrupting efficient CI-MPR trafficking to the *trans*-Golgi.

### Retromer SNX-BARs Restrict *C. trachomatis* Infection

As IncE<sub>101–132</sub> expression altered retromer trafficking, we tested the hypothesis that retromer may be detrimental to *C. trachomatis* infection. Depletion of SNX5/6 or all four retromer SNX-BARs significantly enhanced production of infectious progeny (Figure 7D), suggesting that retromer SNX-BARs restrict *C. trachomatis* infection. While we observed a trend toward enhanced progeny with VPS35 depletion, it did not reach statistical significance ( $p = 0.0574$ ). Enhanced progeny could not be explained by an increase in primary infection; in fact, we noted a significant decrease in primary inclusion formation upon SNX1/2 depletion (Figure 7E). Thus, SNX1/2 may participate in early stages of infection, which could explain the more modest effect of SNX1/2 depletion on infectious progeny production (Figure 7D). Altogether, our results support a model (Figure S7) whereby IncE directly binds SNX5/6, which redirects the retromer SNX-BAR subcomplex to the inclusion membrane, with two functional consequences. First, recruitment of SNX-BARs induces inclusion membrane tubulation, likely through the well-studied ability of BAR domain proteins to induce membrane curvature. Second, by sequestering SNX-BARs at the inclusion and potentially disrupting retromer function, *C. trachomatis* relieves the restriction that retromer imposes on infection.

## DISCUSSION

Assigning functions to individual *Chlamydia* effectors has been difficult in the absence of robust genetic approaches. In this study, we applied an unbiased systematic AP-MS approach to comprehensively identify putative host targets of Incs, effectors that are ideally poised to orchestrate host-pathogen interactions. Our work is especially valuable because very few Inc targets had been identified.

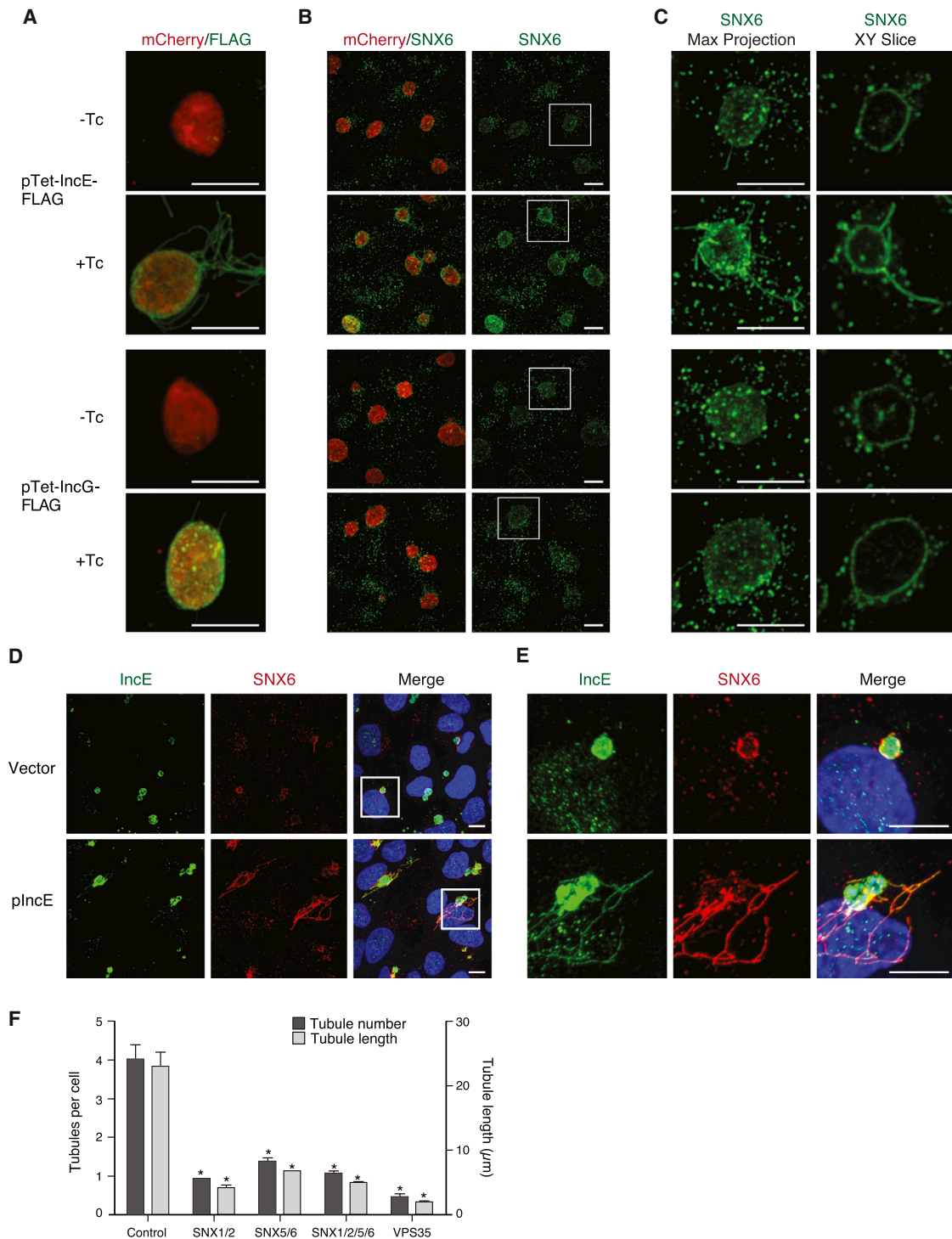


### Figure 6. IncE Is Sufficient to Enhance SNX-BAR Recruitment and Inclusion Tubulation

(A–C) HeLa cells were infected with *C. trachomatis* serovar L2 transformed with pTet-IncE-FLAG or pTet-IncG-FLAG. As indicated, Tc was added at 1 hpi. At 20 hpi, cells were analyzed by confocal microscopy for (A) FLAG or (B and C) SNX6. (A and B) Maximal intensity projections of 0.2  $\mu\text{m}$  z slices. (C) shows maximal intensity projections and single XY slices from the boxed region in (B). Scale bar, 10  $\mu\text{m}$ .

(D and E) HeLa cells were infected with *C. trachomatis* serovar L2 transformed with empty vector or plncE. At 15 hpi, cells were fixed and stained with anti-SNX6, IncE, and DAPI. (E) shows enlargement of boxed region of (D). All images are maximum intensity projections. Scale bar, 10  $\mu\text{m}$ .

(F) Quantitation of inclusion tubules per cell (dark gray bars) and length of the longest tubule per cell (light gray bars) ( $\mu\text{m}$ ) in *C. trachomatis*-infected HeLa cells depleted of the indicated retromer components by siRNA. Data are mean  $\pm$  SEM from three independent experiments. \* $p < 0.001$  compared to corresponding control, unpaired (two-tailed) t test. See also Figure S6.

As with any AP-MS approach, false positives and false negatives are unavoidable. We employed two stringent scoring algorithms, MiST and CompPASS, to minimize false positives. Technical limitations of AP-MS may lead to false negatives (Verschuere et al., 2015), which could explain our failure to identify the following interactions: 14-3-3 $\beta$  and IncG (Scidmore and Hackstadt, 2001), Rab4 and CT229, (Rzomp et al., 2006), or VAMPs and IncA (Delevoeye et al., 2008). Our inability to identify high-confidence PPIs for  $\sim$ 1/3 of IncS could be explained if (1) the Inc serves a structural role in the inclusion membrane (Mital et al., 2013), (2) the host target is a lipid (Mital et al., 2013), or (3) multiple IncS function together to form a binding interface (Gauliard et al., 2015; Mital et al., 2010). Importantly, some putative IncS have not been observed on the inclusion membrane at 24 hpi (Dehoux et al., 2011; Li et al., 2008; summarized in Table S1); however, their localization may be stage, cell type, or serovar specific. Of the 20 IncS whose membrane localization has been experimentally verified (Dehoux et al., 2011; Li et al., 2008), we identified high-confidence host targets for 15 IncS (75%) and validated two published Inc-host interactions (Derré et al., 2011; Lutter et al., 2013). Overall, this Inc-host interactome allows us to link host processes to specific IncS and identifies a plethora of Inc-human interactions of significant biological interest that merit further investigation.

Our standardized AP-MS pipeline provides an unprecedented opportunity to learn whether diverse intracellular pathogens use common strategies to survive. Not only did we observe a significant overlap between the interactomes of *C. trachomatis* and three human viruses, but we found that the more evolutionarily conserved core IncS are more likely to share host targets with viral effectors. Comparison of the overlap among all four pathogens revealed two common targets, MSH2 and UBE2O, suggesting that these host proteins may be critical for intracellular pathogen survival. Modulating UBE2O, one of  $\sim$ 35 human E2 ubiquitin ligases, is particularly intriguing, as it may be an efficient way for intracellular pathogens to regulate the stability of a distinct subset of host proteins.

Our Inc-human PPI network reveals an interaction between IncE and retromer SNX-BARs, which are involved in tubular-based endosomal trafficking (Seaman, 2012). SNX-BAR recruitment to membranes typically involves binding of SNX-PX domains to endosome-specific PtdIns(3)P (Cullen and Carlton, 2012; Seaman, 2012). Our work suggests that SNX5/6 bind directly to IncE independently of phosphoinositides and that the predicted IncE C-terminal  $\beta$ -hairpin is required. Our findings expand the emerging concept that PX domains function not only as lipid recognition modules but also as PPI domains (Teasdale and Collins, 2012). While the molecular details of the IncE-SNX5/6 interaction await further investigation, we note that SNX5/6 contain a unique double PXXP motif with an adjacent  $\sim$ 30 amino acid insertion that forms a long helical hairpin (Koharudin et al., 2009), which distinguishes SNX5/6 from SNX1/2. This feature may contribute to the recognition of SNX5/6 by IncE.

Our data predict that by sequestering SNX-BARs, IncE could disrupt retromer trafficking. To examine retromer trafficking in *Chlamydia*-infected cells, we used an assay that did not directly involve retromer cargo as a readout, since full-length IncE may bind cargo directly (Table S1) and the CI-MPR localizes to the inclusion membrane (van Ooij et al., 1997; our unpublished data).

We examined processing and release of cathepsin D, a secreted lysosomal protease that is missorted when retromer trafficking is disrupted (Rojas et al., 2008). We were unable to demonstrate robust intracellular accumulation of the incompletely processed forms (our unpublished data), as reported upon depletion of VPS26 or Rab7 (Rojas et al., 2008), which could be explained if *Chlamydia* also alters secretory pathways. We do show that ectopic expression of IncE<sub>101–132</sub>, which does not appear to bind cargo (Table S1), alters CI-MPR localization in a manner similar to what is observed upon SNX5/6 depletion (Wassmer et al., 2007).

We observed a profound increase in infectious progeny production upon SNX5/6 depletion, which we postulate recapitulates IncE-mediated recruitment of the SNX-BAR complex away from retromer-containing compartments to the inclusion membrane. As primary inclusion formation was not enhanced, we predict that SNX5/6 restricts *Chlamydia* infection at later steps in the life cycle, such as replication, RB to EB conversion, EB escape, or EB infectivity. While the mechanism by which SNX5/6 restricts bacterial development is not clear, it could be through retromer-dependent or retromer-independent pathways. For example, retromer trafficking may contribute to the recognition or clearance of *Chlamydia*. Alternatively, since retromer is required to maintain the integrity of the *trans*-Golgi (Wassmer et al., 2007), IncE-mediated sequestration of retromer SNX-BARs may promote Golgi fragmentation, a process that facilitates lipid acquisition by *C. trachomatis* and enhances progeny production (Heuer et al., 2009). Finally, SNX5/6 may have other roles outside of retromer trafficking (Sun et al., 2013) that contribute to *Chlamydia* restriction.

Our results provide mechanistic insights into the formation of *Chlamydia* inclusion tubulation. We demonstrate that IncE and SNX-BARs colocalize on the inclusion membrane and tubules, that ectopic expression of IncE is sufficient to induce inclusion tubulation, and that depletion of retromer components limits inclusion tubulation. The direct recruitment of BAR-domain-containing proteins to the inclusion membrane provides a mechanistic link to tubulation, as these proteins are necessary and sufficient for membrane deformation and endosomal tubule formation (Frost et al., 2009). While the role of the tubules is not entirely understood, they are proposed to play a role in secondary inclusion formation (Suchland et al., 2005). We demonstrate that inclusion tubulation and infectious progeny production can be uncoupled: SNX5/6 depletion, which abrogates tubulation, leads to increased infectious progeny.

Our work highlights the strategies employed by diverse intracellular pathogens to repurpose retromer. Silencing of retromer components abrogates HIV (Groppelli et al., 2014), HPV (Lipovsky et al., 2013), *Coxiella* (McDonough et al., 2013), and *Salmonella* (Bujny et al., 2008) infections. Our finding that VPS35 is readily recruited to SCVs reveals that *Salmonella* recruits the VPS complex in addition to retromer SNX-BARs. In contrast, *Chlamydia* IncE selectively recruits retromer SNX-BARs without stably recruiting VPS components or SNX27. Interestingly, through an entirely different mechanism, *Legionella* also disassembles retromer subcomplexes by sequestering VPS components and blocking SNX-PtdIns(3)P binding (Finsel et al., 2013).

In summary, we have applied AP-MS to create a global network of *C. trachomatis* Inc-host PPIs, providing a

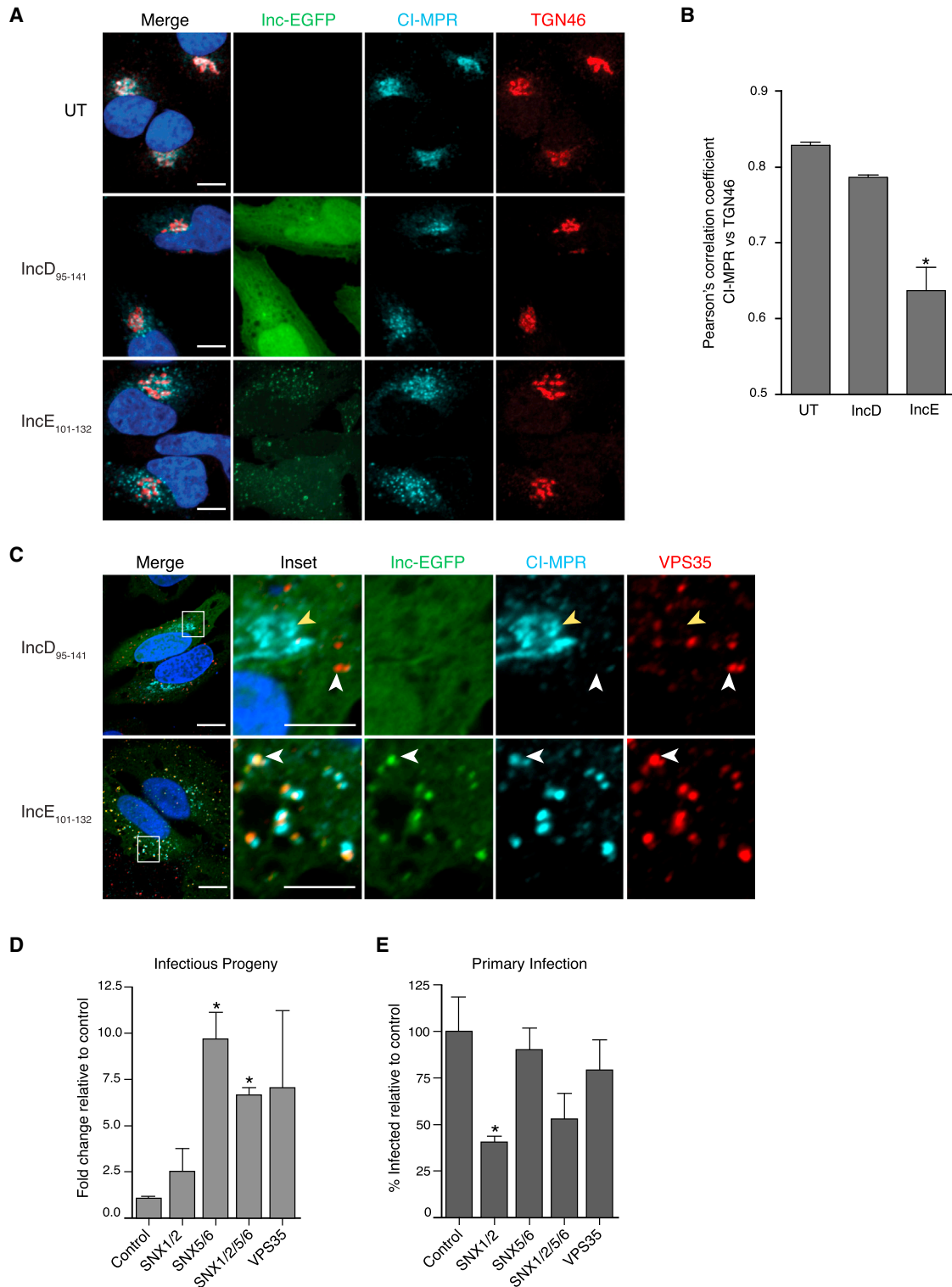


**Figure 7. IncE<sub>101-132</sub>-EGFP Disrupts Retromer Trafficking, and Retromer Depletion Restricts *C. trachomatis* Infection**

(A) Localization of endogenous CI-MPR is perturbed in HeLa cells transiently transfected with IncE<sub>101-132</sub>-EGFP, but not IncD<sub>95-141</sub>-EGFP, compared to untransfected (UT). Cells were fixed and stained with antibodies to TGN46, CI-MPR, and costained with DAPI. Shown are single z slices from confocal images. Scale bar, 10  $\mu$ m.

(B) Quantitation of TGN46 colocalization with CI-MPR in cells expressing IncE<sub>101-132</sub>-EGFP or IncD<sub>95-141</sub>-EGFP. Mean Pearson's correlation coefficients from two independent experiments (n = ~20 cells per experiment). \*p < 0.05 compared to UT or IncD, using one-way ANOVA, post hoc Tukey's test.

(legend continued on next page)

comprehensive bacterial effector-host interactome. Our analysis has uncovered a wealth of previously unidentified *Chlamydia* Inc-host interactions. By linking individual Incs to specific host processes, our work, in conjunction with the development of genetic tools to generate targeted null mutants in *Chlamydia* (Johnson and Fisher, 2013), sets the stage to test the functional role of Incs. This methodology has broad applicability to the study of pathogenesis and is equally effective for identifying the targets of both membrane-bound and soluble effectors. We have uncovered overlapping and potentially druggable pathways targeted by viral and bacterial pathogens. Finally, investigation of the IncE-SNX5/6 interaction may provide insight into retromer biology.

## EXPERIMENTAL PROCEDURES

### Cell Culture, Transformations, and Bacterial Propagation

HeLa and HEK293T cells were maintained under standard conditions. *C. trachomatis* serovar D and L2 were propagated as previously described (Eliwell et al., 2011). *Chlamydia* transformations were performed as previously described (Agaïsse and Derré, 2013; Wang et al., 2013).

### Affinity Purification and Mass Spectrometry

Affinity purifications were performed as previously described (Jäger et al., 2012). Eluates were processed, trypsin digested, and concentrated for LC-MS/MS. Digested peptide mixtures were analyzed on a Thermo Scientific Velos Pro ion trap MS system equipped with a Proxeon Easy nLC II high-pressure liquid chromatography and autosampler system.

### Scoring and Analyzing the Inc-Host Interactome

AP-MS samples were scored with CompPASS (Sowa et al., 2009) and MIST algorithms, using MiST weights optimized for the KSHV-host interactome (Davis et al., 2015). The scored data set included a subset of *Chlamydia* secreted effectors that will be published independently. All bait-prey pairs with a MiST score  $\geq 0.70$  or the top 1% of the CompPASS WD scores were combined with human protein interactions from CORUM and STRING databases that connect prey. The resulting network diagram was plotted using Cytoscape, v.3.1.2 (Smoot et al., 2011). All scored preys were queried against GO, KEGG, and PFAM ontologies for functional and domain annotations. Terms were manually curated, and baits were analyzed for significantly enriched terms with a resampling procedure using MiST scores. Viral overlap was performed as previously described (Davis et al., 2015), and statistical analysis was performed using the hypergeometric test.

### Infections and RNAi

Cells were infected with *Chlamydia* for 1 hr and then incubated for 15–24 hr (primary infection, tubulation or immunoprecipitation) or 72 hr (progeny production). For some experiments, nocodazole or Tc was added 1 hpi. HeLa cells were transfected with siRNAs (Dharmacon) according to manufacturer's protocols and infected with *Chlamydia* at 48 hr. Protein depletion was assayed by immunoblot.

### Transfections and Immunoprecipitations

Lysates from HeLa cells collected 24 hpi were immunoprecipitated with control IgG or anti-SNX6 antibody using Protein G Dynabeads (Invitrogen). Alternatively, HeLa cells were transfected (Effectene, QIAGEN) with the indicated FLAG-SNX construct, infected 24 hr later with *C. trachomatis*, collected at

24 hpi, immunoprecipitated with anti-FLAG beads (Sigma), and eluted with FLAG peptide.

### Microscopy

HeLa cells were grown on glass coverslips, infected with *Chlamydia*, fixed, stained with the indicated primary and fluorophore-conjugated secondary antibodies, and mounted with Vectashield containing DAPI (Vector Laboratories). Images were acquired using Yokogawa CSU-X1 spinning-disk confocal mounted on a Nikon Eclipse Ti inverted microscope equipped with an Andora Clara digital camera. Images were acquired and processed using NIS-Elements software 4.10 (Nikon). Quantitations of tubule number/length and colocalization were performed using Nikon Elements. Inclusions were quantified using the Spot function in Imaris. Statistics were performed using InStat software; p values less than 0.05 were considered statistically significant.

### In Vitro Pull-Downs

Purified 6xHis-MBP-Inc-Strep constructs were immobilized to Strep-Tactin Sepharose beads according to manufacturer's instructions (IBA) and incubated with purified 8xHis-SNX<sub>FX</sub> or 6xHis-MBP-SNX<sub>BAR</sub> domains (1:2 molar ratio), the beads were washed extensively, and the complexes were boiled and analyzed by Coomassie blue staining.

## SUPPLEMENTAL INFORMATION

Supplemental Information includes seven figures, three tables, and Supplemental Experimental Procedures and can be found with this article at <http://dx.doi.org/10.1016/j.chom.2015.06.004>.

## AUTHOR CONTRIBUTIONS

K.M.M., C.A.E., N.J.K., and J.E. conceived, designed, and analyzed experiments. Manuscript was written by K.M.M., C.A.E., and J.E. with input from E.V., J.V.D., J.R.J., I.D., A.M.G., and N.J.K. E.V., J.V.D., J.R.J., N.G., S.J., and T.J. performed MS or bioinformatics analyses. K.M.M., C.A.E., A.F., G.J., T.J., A.M.G., I.D., and J.S. conducted experiments. O.R., R.V., M.N.S., J.D.D., A.O., J.S.C., and B.P. provided reagents or advice. M.S. assisted in figure design and graphics.

## ACKNOWLEDGMENTS

We thank Drs. Deborah Dean, Jai-Jai Liu, Ted Hackstadt, Dan Rockey, Denise Monack, Mark von Zastrow, Sourav Bandyopadhyay, and John Jascur for reagents; the UCSF Biological Imaging Development Center for use of software; and members of the Engel, Krogan, and Sil labs for advice. We acknowledge grant support from NIH (J.E., R01 AI073770, AI105561; N.J.K., P50 GM082250, PO1 AI090935, PO1 090935, P50 GM081879, PO1 091575, U19 AI106754, U54AI081680, DARPA-10-93-Prophecy-PA-008; R.V., AI081694 and AI100759; I.D., R01AI101441; O.R., K08AI091656; B.P., P0065678 A121844 [CA-0063244]), UCSF Microbial Pathogenesis and Host Defense T32 (K.M.M.), American Heart Association (K.M.M.), and the UCSF Program for Breakthrough in Biomedical Research (J.E. and N.K.).

Received: February 24, 2015

Revised: April 28, 2015

Accepted: June 5, 2015

Published: June 25, 2015

(C) CI-MPR remains localized to VPS35-positive compartments in cells expressing IncE<sub>101-132</sub>-EGFP, but not IncD<sub>95-141</sub>-EGFP. HeLa cells were fixed and stained with antibodies to VPS35 and CI-MPR, and costained with DAPI. Shown are single z slices from confocal images. White arrows, VPS35-positive compartment; yellow arrows, CI-MPR-positive compartment. (Left panel) (Merge) Scale bar, 5  $\mu$ m. (Right panels) Enlargements of boxed areas. Scale bar, 2  $\mu$ m.

(D and E) Quantitation of infectious progeny (D) or primary infection (inclusion formation) (E) in HeLa cells infected with *C. trachomatis* serovar D following depletion of the indicated retromer components. Data are mean  $\pm$  SEM from  $\geq 3$  independent experiments. \*p < 0.05 compared to control, unpaired (two-tailed) t test.

## REFERENCES

- Agaisse, H., and Derré, I. (2013). A *C. trachomatis* cloning vector and the generation of *C. trachomatis* strains expressing fluorescent proteins under the control of a *C. trachomatis* promoter. *PLoS ONE* **8**, e57090.
- Arighi, C.N., Hartnell, L.M., Aguilar, R.C., Haft, C.R., and Bonifacino, J.S. (2004). Role of the mammalian retromer in sorting of the cation-independent mannose 6-phosphate receptor. *J. Cell Biol.* **165**, 123–133.
- Bannantine, J.P., Griffiths, R.S., Viratyosin, W., Brown, W.J., and Rockey, D.D. (2000). A secondary structure motif predictive of protein localization to the chlamydial inclusion membrane. *Cell. Microbiol.* **2**, 35–47.
- Bastidas, R.J., Elwell, C.A., Engel, J.N., and Valdivia, R.H. (2013). Chlamydial intracellular survival strategies. *Cold Spring Harb. Perspect. Med.* **3**, a010256.
- Bauer, M.F., Hofmann, S., Neupert, W., and Brunner, M. (2000). Protein translocation into mitochondria: the role of TIM complexes. *Trends Cell Biol.* **10**, 25–31.
- Betts-Hampikian, H.J., and Fields, K.A. (2010). The chlamydial type III secretion mechanism: revealing cracks in a tough nut. *Front Microbiol* **1**, 114.
- Bujny, M.V., Ewels, P.A., Humphrey, S., Attar, N., Jepson, M.A., and Cullen, P.J. (2008). Sorting nexin-1 defines an early phase of *Salmonella*-containing vacuole-remodeling during *Salmonella* infection. *J. Cell Sci.* **121**, 2027–2036.
- Cullen, P.J., and Carlton, J.G. (2012). Phosphoinositides in the mammalian endo-lysosomal network. *Subcell. Biochem.* **59**, 65–110.
- Cullen, P.J., and Korswagen, H.C. (2012). Sorting nexins provide diversity for retromer-dependent trafficking events. *Nat. Cell Biol.* **14**, 29–37.
- Davis, Z.H., Verschuere, E., Jang, G.M., Kleffman, K., Johnson, J.R., Park, J., Von Dollen, J., Maher, M.C., Johnson, T., Newton, W., et al. (2015). Global mapping of herpesvirus-host protein complexes reveals a transcription strategy for late genes. *Mol. Cell* **57**, 349–360.
- Dehoux, P., Flores, R., Dauga, C., Zhong, G., and Subtil, A. (2011). Multi-genome identification and characterization of chlamydiae-specific type III secretion substrates: the Inc proteins. *BMC Genomics* **12**, 109.
- Delevoe, C., Nilges, M., Dehoux, P., Paumet, F., Perrinet, S., Dautry-Varsat, A., and Subtil, A. (2008). SNARE protein mimicry by an intracellular bacterium. *PLoS Pathog.* **4**, e1000022.
- Derré, I., Swiss, R., and Agaisse, H. (2011). The lipid transfer protein CERT interacts with the *Chlamydia* inclusion protein IncD and participates to ER-*Chlamydia* inclusion membrane contact sites. *PLoS Pathog.* **7**, e1002092.
- Elwell, C.A., Jiang, S., Kim, J.H., Lee, A., Wittmann, T., Hanada, K., Melancon, P., and Engel, J.N. (2011). *Chlamydia trachomatis* co-opts GBF1 and CERT to acquire host sphingomyelin for distinct roles during intracellular development. *PLoS Pathog.* **7**, e1002198.
- Finsel, I., Ragaz, C., Hoffmann, C., Harrison, C.F., Weber, S., van Rahden, V.A., Johannes, L., and Hilbi, H. (2013). The *Legionella* effector RidL inhibits retrograde trafficking to promote intracellular replication. *Cell Host Microbe* **14**, 38–50.
- Franceschini, A., Szklarczyk, D., Frankild, S., Kuhn, M., Simonovic, M., Roth, A., Lin, J., Minguez, P., Bork, P., von Mering, C., and Jensen, L.J. (2013). STRING v9.1: protein-protein interaction networks, with increased coverage and integration. *Nucleic Acids Res.* **41**, D808–D815.
- Frost, A., Perera, R., Roux, A., Spasov, K., Destaing, O., Egelman, E.H., De Camilli, P., and Unger, V.M. (2008). Structural basis of membrane invagination by F-BAR domains. *Cell* **132**, 807–817.
- Frost, A., Unger, V.M., and De Camilli, P. (2009). The BAR domain superfamily: membrane-molding macromolecules. *Cell* **137**, 191–196.
- Gauliard, E., Ouellette, S.P., Rueden, K.J., and Ladant, D. (2015). Characterization of interactions between inclusion membrane proteins from *Chlamydia trachomatis*. *Front. Cell. Infect. Microbiol.* **5**, 13.
- Griffiths, E., Ventresca, M.S., and Gupta, R.S. (2006). BLAST screening of chlamydial genomes to identify signature proteins that are unique for the Chlamydiales, Chlamydiaeae, Chlamydiales and Chlamydia groups of species. *BMC Genomics* **7**, 14.
- Groppelli, E., Len, A.C., Granger, L.A., and Jolly, C. (2014). Retromer regulates HIV-1 envelope glycoprotein trafficking and incorporation into virions. *PLoS Pathog.* **10**, e1004518.
- Heuer, D., Rejman Lipinski, A., Machuy, N., Karlas, A., Wehrens, A., Siedler, F., Brinkmann, V., and Meyer, T.F. (2009). *Chlamydia* causes fragmentation of the Golgi compartment to ensure reproduction. *Nature* **457**, 731–735.
- Hong, Z., Yang, Y., Zhang, C., Niu, Y., Li, K., Zhao, X., and Liu, J.J. (2009). The retromer component SNX6 interacts with dynactin p150(Glued) and mediates endosome-to-TGN transport. *Cell Res.* **19**, 1334–1349.
- Jäger, S., Cimermancic, P., Gulbahce, N., Johnson, J.R., McGovern, K.E., Clarke, S.C., Shales, M., Mercenne, G., Pache, L., Li, K., et al. (2012). Global landscape of HIV-human protein complexes. *Nature* **481**, 365–370.
- Johnson, C.M., and Fisher, D.J. (2013). Site-specific, insertional inactivation of *incA* in *Chlamydia trachomatis* using a group II intron. *PLoS ONE* **8**, e83989.
- Koharudin, L.M., Furey, W., Liu, H., Liu, Y.J., and Gronenborn, A.M. (2009). The phox domain of sorting nexin 5 lacks phosphatidylinositol 3-phosphate (PtdIns(3)P) specificity and preferentially binds to phosphatidylinositol 4,5-bisphosphate (PtdIns(4,5)P<sub>2</sub>). *J. Biol. Chem.* **284**, 23697–23707.
- Lauffer, B.E., Melero, C., Temkin, P., Lei, C., Hong, W., Kortemme, T., and von Zastrow, M. (2010). SNX27 mediates PDZ-directed sorting from endosomes to the plasma membrane. *J. Cell Biol.* **190**, 565–574.
- Leonard, C.A., and Borel, N. (2014). Chronic chlamydial diseases: from atherosclerosis to urogenital infections. *Curr. Clin. Micro Rpt.* **1**, 61–72.
- Li, Z., Chen, C., Chen, D., Wu, Y., Zhong, Y., and Zhong, G. (2008). Characterization of fifty putative inclusion membrane proteins encoded in the *Chlamydia trachomatis* genome. *Infect. Immun.* **76**, 2746–2757.
- Lipovsky, A., Popa, A., Pimienta, G., Wyler, M., Bhan, A., Kuruvilla, L., Guie, M.A., Poffenberger, A.C., Nelson, C.D., Atwood, W.J., and DiMaio, D. (2013). Genome-wide siRNA screen identifies the retromer as a cellular entry factor for human papillomavirus. *Proc. Natl. Acad. Sci. USA* **110**, 7452–7457.
- Lutter, E.I., Martens, C., and Hackstadt, T. (2012). Evolution and conservation of predicted inclusion membrane proteins in chlamydiae. *Comp. Funct. Genomics* **2012**, 362104.
- Lutter, E.I., Barger, A.C., Nair, V., and Hackstadt, T. (2013). *Chlamydia trachomatis* inclusion membrane protein CT228 recruits elements of the myosin phosphatase pathway to regulate release mechanisms. *Cell Rep.* **3**, 1921–1931.
- Mandell, G.L., Bennett, J.E., and Dolin, R. (2010). *Mandell, Douglas, and Bennett's Principles and Practice of Infectious Diseases* (Philadelphia: Churchill Livingstone/Elsevier), p. 1, online resource.
- Marshansky, V., and Futai, M. (2008). The V-type H<sup>+</sup>-ATPase in vesicular trafficking: targeting, regulation and function. *Curr. Opin. Cell Biol.* **20**, 415–426.
- McDonough, J.A., Newton, H.J., Klum, S., Swiss, R., Agaisse, H., and Roy, C.R. (2013). Host pathways important for *Coxiella burnetii* infection revealed by genome-wide RNA interference screening. *MBio* **4**, e00606–e00612.
- Mital, J., Miller, N.J., Fischer, E.R., and Hackstadt, T. (2010). Specific chlamydial inclusion membrane proteins associate with active Src family kinases in microdomains that interact with the host microtubule network. *Cell. Microbiol.* **12**, 1235–1249.
- Mital, J., Miller, N.J., Dorward, D.W., Dooley, C.A., and Hackstadt, T. (2013). Role for chlamydial inclusion membrane proteins in inclusion membrane structure and biogenesis. *PLoS ONE* **8**, e63426.
- Moore, E.R., and Ouellette, S.P. (2014). Reconceptualizing the chlamydial inclusion as a pathogen-specified parasitic organelle: an expanded role for Inc proteins. *Front. Cell. Infect. Microbiol.* **4**, 157.
- Olive, A.J., Haff, M.G., Emanuele, M.J., Sack, L.M., Barker, J.R., Elledge, S.J., and Starnbach, M.N. (2014). *Chlamydia trachomatis*-induced alterations in the host cell proteome are required for intracellular growth. *Cell Host Microbe* **15**, 113–124.
- Ramage, H.R., Kumar, G.R., Verschuere, E., Johnson, J.R., Von Dollen, J., Johnson, T., Newton, B., Shah, P., Horner, J., Krogan, N.J., and Ott, M. (2015). A combined proteomics/genomics approach links hepatitis C virus infection with nonsense-mediated mRNA decay. *Mol. Cell* **57**, 329–340.

- Roan, N.R., and Starnbach, M.N. (2006). Antigen-specific CD8+ T cells respond to *Chlamydia trachomatis* in the genital mucosa. *J. Immunol.* *177*, 7974–7979.
- Rockey, D.D., Scidmore, M.A., Bannantine, J.P., and Brown, W.J. (2002). Proteins in the chlamydial inclusion membrane. *Microbes Infect.* *4*, 333–340.
- Rojas, R., van Vlijmen, T., Mardones, G.A., Prabhu, Y., Rojas, A.L., Mohammed, S., Heck, A.J., Raposo, G., van der Sluijs, P., and Bonifacino, J.S. (2008). Regulation of retromer recruitment to endosomes by sequential action of Rab5 and Rab7. *J. Cell Biol.* *183*, 513–526.
- Ruepp, A., Waegel, B., Lechner, M., Brauner, B., Dunger-Kaltenbach, I., Fobo, G., Frishman, G., Montrone, C., and Mewes, H.W. (2010). CORUM: the comprehensive resource of mammalian protein complexes—2009. *Nucleic Acids Res.* *38*, D497–D501.
- Rzomp, K.A., Moorhead, A.R., and Scidmore, M.A. (2006). The GTPase Rab4 interacts with *Chlamydia trachomatis* inclusion membrane protein CT229. *Infect. Immun.* *74*, 5362–5373.
- Scidmore, M.A., and Hackstadt, T. (2001). Mammalian 14-3-3 $\beta$  associates with the *Chlamydia trachomatis* inclusion membrane via its interaction with IncG. *Mol. Microbiol.* *39*, 1638–1650.
- Scidmore-Carlson, M.A., Shaw, E.I., Dooley, C.A., Fischer, E.R., and Hackstadt, T. (1999). Identification and characterization of a *Chlamydia trachomatis* early operon encoding four novel inclusion membrane proteins. *Mol. Microbiol.* *33*, 753–765.
- Seaman, M.N. (2012). The retromer complex - endosomal protein recycling and beyond. *J. Cell Sci.* *125*, 4693–4702.
- Sisko, J.L., Spaeth, K., Kumar, Y., and Valdivia, R.H. (2006). Multifunctional analysis of *Chlamydia*-specific genes in a yeast expression system. *Mol. Microbiol.* *60*, 51–66.
- Smoot, M.E., Ono, K., Ruscheinski, J., Wang, P.L., and Ideker, T. (2011). Cytoscape 2.8: new features for data integration and network visualization. *Bioinformatics* *27*, 431–432.
- Sowa, M.E., Bennett, E.J., Gygi, S.P., and Harper, J.W. (2009). Defining the human deubiquitinating enzyme interaction landscape. *Cell* *138*, 389–403.
- Suchland, R.J., Rockey, D.D., Weeks, S.K., Alzhanov, D.T., and Stamm, W.E. (2005). Development of secondary inclusions in cells infected by *Chlamydia trachomatis*. *Infect. Immun.* *73*, 3954–3962.
- Sun, Y., Hedman, A.C., Tan, X., Schill, N.J., and Anderson, R.A. (2013). Endosomal type I $\gamma$  PIP 5-kinase controls EGF receptor lysosomal sorting. *Dev. Cell* *25*, 144–155.
- Teasdale, R.D., and Collins, B.M. (2012). Insights into the PX (phox-homology) domain and SNX (sorting nexin) protein families: structures, functions and roles in disease. *Biochem. J.* *441*, 39–59.
- van Ooij, C., Apodaca, G., and Engel, J. (1997). Characterization of the *Chlamydia trachomatis* vacuole and its interaction with the host endocytic pathway in HeLa cells. *Infect. Immun.* *65*, 758–766.
- Verschueren, E., Von Dollen, J., Cimermancic, P., Gulbahce, N., Sali, A., and Krogan, N.J. (2015). Scoring large-scale affinity purification mass spectrometry datasets with MiST. *Curr. Protoc. Bioinformatics* *49*, 8 19 11–18 19 16.
- Wang, Y., Kahane, S., Cutcliffe, L.T., Skilton, R.J., Lambden, P.R., Persson, K., Bjartling, C., and Clarke, I.N. (2013). Genetic transformation of a clinical (genital tract), plasmid-free isolate of *Chlamydia trachomatis*: engineering the plasmid as a cloning vector. *PLoS ONE* *8*, e59195.
- Wassmer, T., Attar, N., Bujny, M.V., Oakley, J., Traer, C.J., and Cullen, P.J. (2007). A loss-of-function screen reveals SNX5 and SNX6 as potential components of the mammalian retromer. *J. Cell Sci.* *120*, 45–54.